The phosphatidyl-myo-inositol anchor of the lipoarabinomannans from Mycobacterium bovis bacillus Calmette Guérin. Heterogeneity, structure, and role in the regulation of cytokine secretion.

J. Nigou, M. Gilleron, B. Cahuzac, J. D. Bounéry, M. Herold, M. Thurnher, G. Puzo

THE JOURNAL OF BIOLOGICAL CHEMISTRY
Vol. 272, No. 37, Issue of September 12, pp. 23094–23103, 1997
Printed in U.S.A.

The Phosphatidyl-*myo*-inositol Anchor of the Lipoarabinomannans from *Mycobacterium bovis* Bacillus Calmette Guérin

HETEROGENEITY, STRUCTURE, AND ROLE IN THE REGULATION OF CYTOKINE SECRETION*

(Received for publication, May 29, 1997, and in revised form, June 30, 1997)

Jérôme Nigou‡, Martine Gilleron‡, Bertrand Cahuzac‡, Jean-Dominique Bounéry‡, Manfred Herold§, Martin Thurnher¶, and Germain Puzo‡‖

From the ‡Institut de Pharmacologie et de Biologie Structurale du Centre National de la Recherche Scientifique, 118 route de Narbonne, 31062 Toulouse Cedex, France, the ¶Department of Urology, University of Innsbruck, Anichstrasse 35, 6020 Innsbruck, Austria, and the §Department of Internal Medicine, University of Innsbruck, Anichstrasse 35, 6020 Innsbruck, Austria

Lipoarabinomannans are major mycobacterial antigens capable of modulating the host immune response; however, the molecular basis underlying the diversity of their immunological properties remain an open question. In this study a new extraction and purification approach was successfully applied to isolate ManLAMs (lipoarabinomannans with mannosyl extensions) from bacillus Calmette Guérin leading to the obtention of two types of ManLAMs namely parietal and cellular. Structurally, they were found to differ by the percentage of mannooligosaccharide caps, 76 and 48%, respectively, and also, thanks to a new analytical method, by the structure of the phosphatidyl-*myo*-inositol anchor lipid moiety. A novel fatty acid in the mycobacterium genus assigned to a 12-*O*-(methoxypropanoyl)-12-hydroxystearic acid was the only fatty acid esterifying C-1 of the glycerol residue of the parietal ManLAMs, while the phosphatidyl unit of the cellular ManLAMs showed a large heterogeneity due to a combination of palmitic and tuberculostearic acid. Finally, parietal and cellular ManLAMs were found to differentially affect interleukin-8 and tumor necrosis factor-α secretion from human dendritic cells. We show that parietal but not cellular ManLAMs were able to stimulate tumor necrosis factor-α secretion from dendritic cells. From these studies we propose that the 1-[12-*O*-(methoxypropanoyl)-12-hydroxystearoyl]-*sn*-glycerol part is the major cytokine-regulating component of the ManLAMs. It seems likely that modification of the ManLAM lipid part, which may occur in hostile environments, could regulate macrophagic mycobacterial survival by altering cytokine stimulation.

Tuberculosis remains the leading cause of human death among the infectious diseases with over 3 million deaths each year (1). The decline in tuberculosis in the developed countries has been reversed by the tuberculosis cases arising in AIDS patients, among the homeless, and by the emergence of *Mycobacterium tuberculosis* strains resistant to the first-line drugs, which are isoniazid and ethambutol. Also, from different trials, the efficiency of BCG[1] vaccine to prevent tuberculosis was found to range from 0 to 80% (2, 3).

Virulent mycobacteria survive and multiply within phagosomes of mononuclear phagocytes. Despite conflicting results, there is a consensus that phagosomes containing *M. tuberculosis* do not fuse with lysosomes and resist acidification (4). This survival can also be correlated with the macrophage bactericide activity, which appears to be modulated by mycobacterial cell wall components (5, 6).

From a molecular point of view, cell wall lipoarabinomannans (LAMs) are clearly demonstrated to be pivotal mycobacterial antigens. They regulate TNF-α production by phagocyte (5) and block the transcriptional activation of INF-γ (6), thereby influencing the intramacrophagic survival of mycobacteria. For instance, LAMs (PI-GAMs) from *Mycobacterium smegmatis*, a fast growing mycobacterium that does not survive inside the macrophages, were found to stimulate phagocyte TNF-α production (7), whereas LAMs (ManLAMs) from the pathogenic *M. tuberculosis* Erdman strain, which survives in the macrophages, have much a lower stimulatory activity (5). ManLAMs were found to be endowed with other immunological activities. They selectively bind murine and human phagocytes via the mannose receptor and mediate the adhesion of pathogenic *M. tuberculosis* strains to this receptor (8, 9). In addition, ManLAMs from *Mycobacterium leprae* and *M. tuberculosis* Erdman strains were found to be presented in the context of CD1 molecules and stimulate CD4/CD8 double negative $\alpha\beta$T cells (10).

There is a general consensus that the ManLAMs isolated from BCG (11), *M. tuberculosis* (12, 13), and *M. leprae* (14) share the same basic structure characterized by the following features: a phosphatidyl-*myo*-inositol anchor, a mannan core, an arabinan domain, and mannooligosaccharide caps. Nevertheless, ManLAMs from *M. leprae* and *M. tuberculosis* were found to stimulate T cell clones with different fine specificities

* This work was supported by grants from the Région Midi-Pyrénées (RECH/9307911), from the Mission Scientifique et Technique du Ministère de l'Education Nationale, de l'Enseignement Supérieur et de la Recherche (ACC SV6 9506005), and from the Austrian Science Foundation (to M. T.) (P11758-Med). The costs of publication of this article were defrayed in part by the payment of page charges. This article must therefore be hereby marked "*advertisement*" in accordance with 18 U.S.C. Section 1734 solely to indicate this fact.

‖ To whom correspondence should be addressed. Tel.: 33-5-61-33-59-10; Fax: 33-5-61-33-59-12; E-mail: germain@ipbs.fr.

[1] The abbreviations used are: BCG, bacillus Calmette Guérin; AMs, arabinomannans; APTS, 1-aminopyrene-3,6,8-trisulfonate; CI, chemical ionization; C_{15}, pentadecanoic acid; C_{16}, palmitic acid; C_{18}, stearic acid; C_{19}, tuberculostearic acid; DCs, dendritic cells; LAMs, lipoarabinomannans; ManLAMs, LAMs with mannosyl extensions; dManLAMs, deacylated ManLAMs; EI, electron impact; GC, gas chromatography; GC/MS, gas chromatography coupled to mass spectrometry; GM-CSF, granulocytes/macrophages-colony stimulating factor; HMQC, heteronuclear multiple quantum correlation spectroscopy; HOHAHA, homonuclear Hartmann-Hahn spectroscopy; IL, interleukin; ManAMs, arabinomannans with mannosyl extensions; LMs, lipomannans; PI anchor, phosphatidyl-*myo*-inositol anchor; PI-GAMs, phosphoinositol-glyceroarabinomannans; PAGE, polyacrylamide gel electrophoresis; TMS, trimethylsilyl; TNF, tumor necrosis factor.

(10). This phenomenon remains unclear, even if it was claimed that it arises from the mannooligosaccharide caps frequency (10). This paradoxical situation can be tentatively explained by the fact that structural and functional ManLAMs studies were conducted on complex mixtures. This was revealed by matrix-assisted laser desorption/ionization mass spectrometry studies establishing an average ManLAM molecular mass of 17 kDa and giving a molecular heterogeneity estimated at 6 kDa (11). Moreover the structural analysis of the ManLAMs from *Mycobacterium bovis* BCG revealed that around 50% of the mannan cores were devoid of the expected phosphatidyl-*myo*-inositol anchor, suggesting that the analyzed fraction, containing arabinose and mannose, was a mixture of lipoglycans and glycans (15).

We report here a new strategy to extract ManLAMs from *M. bovis* BCG, which can be extended to the LAMs from other mycobacterial strains. The protocol enables the isolation of two types of ManLAMs, namely parietal and cellular (16). In addition, a new purification method was successfully developed allowing the separation of glycans from lipoglycans. We demonstrate that cellular and parietal ManLAMs differ by their PI anchor structure and by the frequency of the mannooligosaccharide caps. Drastic differences were also observed in their capacity to stimulate cytokine secretion from human dendritic cells (DCs).

MATERIALS AND METHODS

ManLAMs Extraction and Purification—As explained in Fig. 1, *M. bovis* BCG Pasteur strain cells were delipidated using $CHCl_3/CH_3OH$, 1:1, v/v. The delipidated mycobacteria were extracted six times by refluxing in 50% ethanol at 65 °C for 8 h. The resulting cells were washed and disintegrated in ice by sonication (20 kHz, 600 watts, 15 min) and using a French pressure cell (one step of lysis at a pressure maintained above 200 megapascals). The ethanol/water extracts (parietal fraction) were dried, incubated in 2% Triton X-100 (Sigma), and dialyzed against it to eliminate most of the hydrophobic molecules such as phosphatidyl-*myo*-inositol mannosides. Triton X-100 was removed by a partition $CHCl_3/CH_3OH/H_2O$, 2:1:1, v/v/v. The water-soluble fraction containing lipoglycans, glycans, and proteins was treated with both enzymes, trypsin (from bovine pancreas, Sigma) and α-amylase (from *Bacillus amyloliquefaciens*, Boehringer Mannheim GmbH), and dialyzed against water. Most of the proteins of the cellular fraction were removed by a hot 80% (w/w) aqueous phenol biphasic wash at 70 °C for 1 h. After enzymatic treatments by trypsin, α-amylase, RNase A (from bovine pancreas, Sigma), and DNase I (from bovine pancreas, Fluka), a step of dialysis removed the amino acids, glucose, nucleotides, and phenol from the cellular glycans and lipoglycans. Triton X-114 phase separation technique was applied on glycan and lipoglycan mixtures (see below). ManLAMs and LMs were then separated by gel filtration. Sample (60 mg) was dissolved in 0.2 M NaCl, 0.25% sodium deoxycholate (w/v), 1 mM EDTA and 10 mM Tris, pH = 8, to a final concentration of 200 mg/ml, incubated 2 days at room temperature, and loaded on a gel permeation Bio-Gel P-100 column (52 × 3 cm) eluted with the same buffer at a flow rate of 5 ml/h. SDS-PAGE was performed as described by Venisse *et al.* (11).

Triton X-114 Phase Separation Method—As described by Bordier (17), three precondensations of commercial Triton X-114 (Sigma) were performed leading to a concentration of Triton X-114 in the detergent-rich phase of 13.2% (w/v), corresponding to the stock solution. The ManLAM containing fractions were dissolved in water (1 mg/ml final volume), and Triton X-114 stock solution was added to a final concentration of Triton X-114 of 2% (w/v). The mixture was homogenized at 4 °C for 1 h and then incubated at 37 °C to allow separation into the detergent-rich and the detergent-depleted phases, the latter being collected. To optimize the fractionation between the glycans and the lipoglycans, these two phases were again homogenized by adding either water or Triton X-114 stock solution to a final Triton concentration of 2% and again separated. This process was repeated twice leading to four detergent-rich and four detergent-depleted phases, which were respectively pooled. From both phases, the Triton X-114 was mainly removed by extraction with $CHCl_3$ (controlled by UV (17)), the resulting aqueous phases were dried and addition of absolute ethanol led to the precipitation of lipoglycans and glycans.

Chemical Analysis—Carbohydrates and inositol were analyzed as their trimethylsilyl glycosides dissolved in cyclohexane after hydrolysis with 0.6 N HCl, 110 °C, 1 h.

Glycosyl linkage composition was analyzed after methylation of polysaccharides according to the modified procedure from Ciucanu and Kerek (18). The methylated polysaccharides were hydrolyzed with 2 N trifluoroacetic acid at 110 °C for 2 h, reduced with $NaBD_4$ 10 mg/ml in NH_4OH 1 M/C_2H_5OH, 1:1, v/v, freshly prepared and peracetylated with acetic anhydride 1 h at 110 °C. The alditol acetates were solubilized in cyclohexane before injection in gas chromatography (GC) and gas chromatography coupled to mass spectrometry (GC/MS).

Fatty acids were analyzed as their methyl esters. ManLAMs were deacylated in 1 N NaOH, 37 °C, 2 h, and then neutralized with HCl. Fatty acids were extracted using cyclohexane/water, 1:1, v/v, and after drying under N_2, were methylated with 10% (w/w) BF_3 in methanol (Fluka) at 60 °C for 5 min. Reaction was stopped by addition of water, and fatty acid methyl esters were extracted as described above before injection in GC and GC/MS. Pentadecanoic acid was used as internal standard. Phosphorus was measured for the determination of the molar ratio of fatty acids to phosphorus by the procedure described by Schnitger *et al.* (19).

Acetolysis Procedure—3 mg of ManLAMs were treated with 400 μl of anhydrous acetic acid/acetic anhydride, 3:2, v/v, at 110 °C for 12 h (20). The reaction mixture was dried and vortexed with 400 μl of cyclohexane/water, 1:1, v/v. The cyclohexane phase was analyzed by GC/MS.

GC and GC/MS Analysis—GC was performed on a Girdel series 30 equipped with an OV1 capillary column (0.22 mm × 25 m) using helium gas with a flow rate of 2.5 ml/min with a flame ionization detector at 310 °C. The injector temperature was 260 °C, and the temperature separation program was from 100 to 290 °C at a speed of 3 °C/min. GC/MS analysis were performed on a Hewlett-Packard 5889 X mass spectrometer (electron energy, 70 eV) working on both electron impact (EI) and chemical ionization modes using NH_3 as reagent gas (CI/NH_3), coupled with a Hewlett-Packard 5890 gas chromatograph series II fitted with a similar OV1 column (0.30 mm × 12 m). Acetolysis products were analyzed on a 0.35-m length column using a temperature separation program from 160 to 300 °C at a speed of 8 °C/min. The injector and interface temperatures were 290 °C.

Capillary Electrophoresis—Analyses were performed on a P/ACE capillary electrophoresis system (Beckman Instruments, Inc.) with the cathode on the injection side and the anode on the detection side. The electropherograms were acquired and stored on a Dell XPS P60 computer using the System Gold software package (Beckman Instruments, Inc.).

2 μg of dried mild hydrolyzed (0.1 N HCl at 110 °C for 30 min) ManLAMs were mixed with 0.5 μl of 0.2 M 1-aminopyrene-3,6,8-trisulfonate (APTS) (eCAP *N*-Linked oligosaccharides profiling kit, Beckman Instruments, Inc.) in 15% acetic acid and 0.5 μl of a 1 M sodium cyanoborohydride solution dissolved in tetrahydrofuran (Aldrich) (21). The reaction was performed 90 min at 55 °C, and the samples were then diluted in 9 μl of water before injection. APTS derivatives were loaded by applying 0.5 p.s.i. (3.45 kPa) vacuum for 5 s. Separations were performed using a coated capillary column (eCAP N-CHO coated capillary from eCAP *N*-Linked oligosaccharides profiling kit, Beckman Instruments, Inc.) of 50 μm internal diameter with 40 cm effective length (47 cm total length). Analyses were carried out at a temperature of 20 °C with an applied voltage of 24 kV and using degassed carbohydrate separation gel buffer (eCAP *N*-Linked oligosaccharides profiling kit, Beckman Instruments, Inc.) as running electrolyte. Detection system consisted in a Beckman laser-induced fluorescence equipped with a 4-milliwatt argon-ion laser with the excitation wavelength of 488 nm and emission wavelength filter of 520 nm.

NMR Spectroscopy—NMR spectra were recorded on a Bruker AMX-500 spectrometer equipped with an Aspect X32 computer. Samples were exchanged in D_2O (Spin et Techniques, Paris, 99.9% purity) with intermediate lyophilization, then dissolved in 99.96 atom % D_2O and analyzed in 200 × 5-mm 535-PP NMR tubes. The concentration of the NMR samples were 40 mg/ml for parietal ManLAMs and 120 mg/ml for cellular ManLAMs. Spectra were recorded at 313 K. The ^1H NMR chemical shifts were referenced relative to internal acetone signal at 2.225 ppm.

The one-dimensional phosphorus (^{31}P) spectra were measured at 202.46 MHz by employing a spectral width of 25 kHz, and phosphoric acid (85%) was used as the external standard (δ_P 0.0). The data were collected in 32,768 complex data sets, and an exponential transformation (LB = 5 Hz) was applied prior the processing to 65,536 real points in the frequency domain. The spectrum was recorded with 64 scans for parietal ManLAMs and 512 scans for cellular ManLAMs.

The two-dimensional ^1H-^{31}P HMQC-HOHAHA spectra were recorded without sample spinning in the proton-detected mode with a Bruker 5-mm ^1H broad band tunable probe with reversal geometry using the Lerner and Bax pulse sequence (22). The GARP sequence (23)

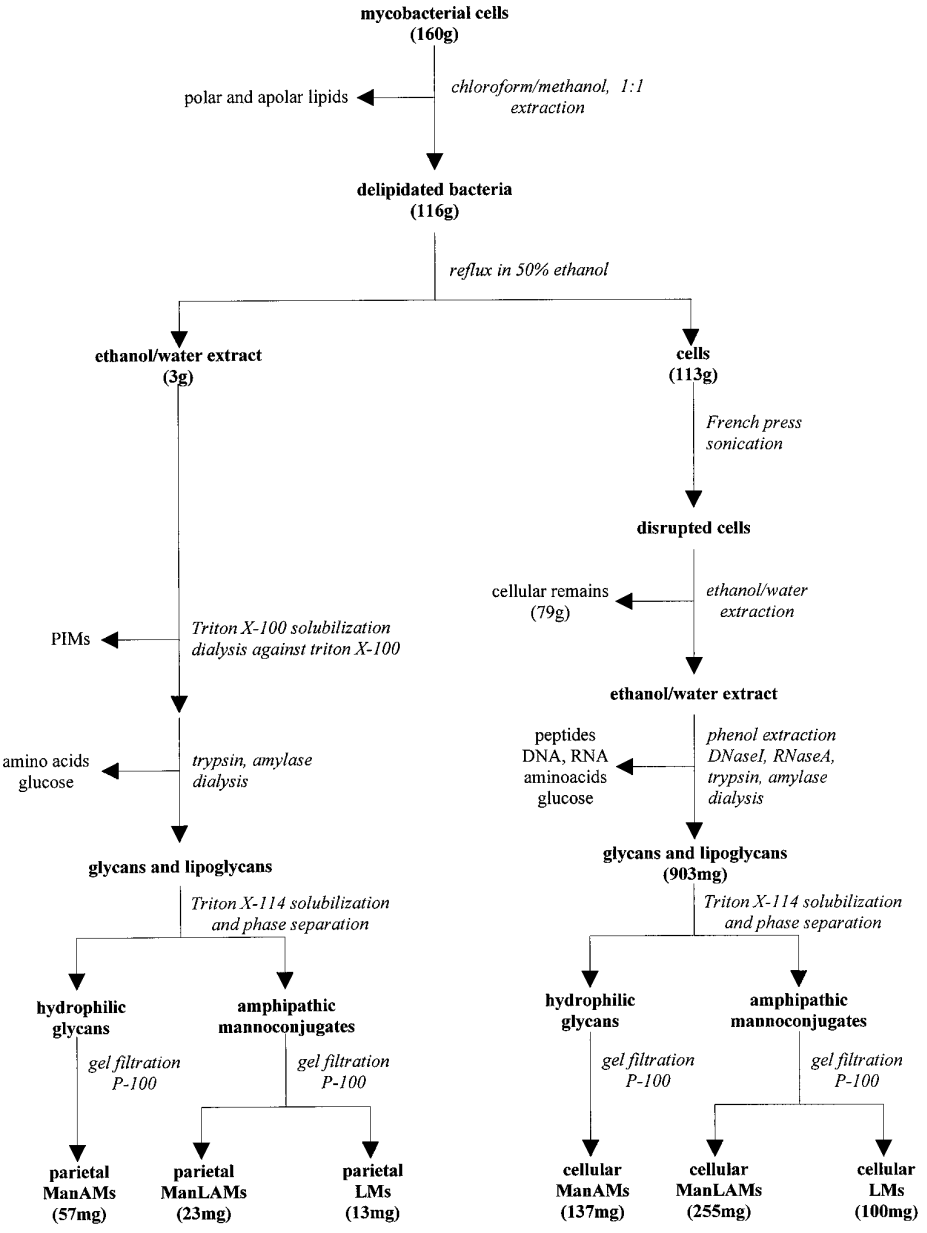

FIG. 1. **Purification scheme for the parietal and cellular ManLAMs and related compounds from *M. bovis* BCG Pasteur strain.**

at the carbon frequency was used as a composite pulse decoupling during acquisition. Data were acquired in the phase-sensitive mode using the time-proportional phase increment method (24). For parietal ManLAMs, spectral widths of 607.38 Hz in ^{31}P and 5005 Hz in ^{1}H dimensions were used to collect a 4096 × 42 (time-proportional phase increment) point data matrix with 108 scans/t_1 value expanded to 4096 × 1024 by zero filling. The mixing time was 34 ms. For parietal deacylated ManLAMs, spectral widths of 10 123 Hz in ^{31}P and 4003 Hz in ^{1}H dimensions were used to collect a 4096 × 128 (time-proportional phase increment) point data matrix with 96 scans/t_1 value expanded to 4096 × 1024 by zero filling. The mixing time was 63 ms. In both case, the relaxation delay was 1 s, and a sine bell window shifted by $\pi/2$ was applied in both dimensions.

Cell Culture Media and Cytokines—The medium used in this study was RPMI 1640 with 1% heat-inactivated (30 min, 56 °C) pooled human AB serum, 50 units/ml penicillin, 50 μg/ml streptomycin, 2.5 μg/ml fungizone, 2 mM L-glutamine, 10 mM Hepes, 0.1 mM non-essential amino acids, 1 mM pyruvate, and 5×10^{-5} M 2-mercaptoethanol (all from Boehringer Ingelheim Bioproducts, Vienna, Austria). Human albumin (for intravenous use; Octopharma, Vienna, Austria) was added to a final concentration of 2 mg/ml (=complete medium). Recombinant GM-CSF (Leucomax; 1.11×10^7 units/mg) was from Sandoz (Basel, Switzerland). Recombinant human IL-4 (2×10^7 units/mg) was kindly supplied by the Schering-Plough Research Institute (Kenilworth, NJ).

DCs and Quantitation of Cytokines—Cultures of human DCs were established as described (25). Briefly, mononuclear cells were obtained by standard density gradient centrifugation on Ficoll-Paque (Pharmacia Biotech Inc., Uppsala, Sweden). The adherent fraction (45 min, 37 °C) was cultured in complete medium containing 1000 units/ml each GM-CSF and IL-4. Every other day, one-third of the medium was replaced by fresh medium containing GM-CSF/IL-4. DCs were routinely used at day 6. After extensive washing, the cells were recultured at 10^5 cells/ml with or without ManLAMs at the indicated concentrations. Supernatants were harvested for IL-8 and TNF-α assays after 6 h. The enzyme-linked immunosorbent assay was carried out with a commercially available kit from CLB (Amsterdam, The Netherlands) specific for IL-8 and TNF-α. Cytokines were quantitated using a microtiter plate reader.

RESULTS

Extraction and Purification of ManLAMs

The presence of ManLAMs, namely parietal ManLAMs, in ethanol/water extracts from delipidated BCG Pasteur strain cells was unambiguously established by routine carbohydrate analysis revealing the occurrence of arabinose and mannose. This assumption was also supported by SDS-PAGE analysis showing a characteristic broad band at 30 kDa. As outlined in the purification scheme (Fig. 1), the resulting cells were dis-

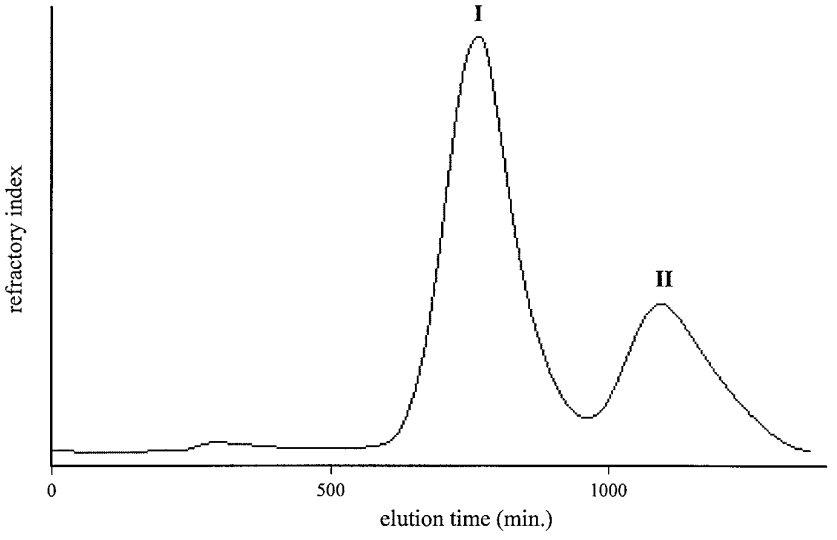

FIG. 2. **Bio-Gel P-100 gel filtration chromatogram of the fraction containing parietal ManLAMs and LMs.** The fraction was loaded on a Bio-Gel P-100 column (52 × 3 cm), eluted with 0.2 M NaCl, 0.25% sodium deoxycholate (w/v), 1 mM EDTA, and 10 mM Tris, pH = 8, and monitored by refractory index. *Peaks I* and *II* were assigned to ManLAMs and LMs, respectively, from SDS-PAGE analysis. Cellular lipoglycans show the same chromatographic profile than the parietal ones.

rupted and extracted again by an ethanol/water mixture. This extract, analyzed as mentioned above for the parietal extract, was found again to contain ManLAMs: namely cellular ManLAMs (16).

The fraction containing parietal ManLAMs was submitted to the following process: i) incubation in 2% Triton X-100 and dialysis against it to remove the phosphatidyl-*myo*-inositol mannosides, ii) elimination of the Triton X-100 by partition, iii) enzymatic hydrolysis by trypsin and α-amylase to remove the protein and glucan contaminants. At the end of this process, the parietal ManLAM fraction was still contaminated by amphipathic glycoconjugates like LMs and the expected glycans such as arabinomannans (AMs) and mannans.

Besides the different contaminants (proteins, glucans) described above for the parietal ManLAM fraction, DNA and RNA were also present in the cellular ManLAM fraction. All these contaminants were enzymatically removed. To eliminate the glycans from the parietal and cellular ManLAM fractions, the Triton X-114 phase separation method, which is summarized below, was successfully applied.

Triton X-114 forms a clear micellar solution at 4 °C and two phases at 22 °C, a hydrophilic detergent-depleted phase and an amphipathic detergent-rich phase. The ManLAM fractions were dissolved in water (1 mg/ml final volume) and then preconditioned Triton X-114 stock solution (17) was added to a final concentration of 2% Triton X-114 (w/v). The mixture was homogenized at 4 °C for 1 h, then incubated at 37 °C giving two phases, *i.e.* the detergent-rich and the detergent-depleted phases, the latter being collected. To optimize fractionation between the glycans and the lipoglycans, the two phases were both treated again twice. From SDS-PAGE analysis, using ManLAM and LM standards, it was deduced that the parietal and cellular mannoglycoconjugates which are soluble in the detergent-rich phase correspond to a mixture of ManLAMs and LMs. The parietal and cellular detergent-depleted phases were analyzed in the same way and from the absence of migration on the gel, the compounds were assigned to glycans. They were definitively identified, after Bio-Gel P-100 gel filtration, by routine carbohydrate analysis (Ara/Man = 1.2 and 1.7 for the parietal and cellular glycans respectively) as AMs. Thus, by means of the Triton X-114 method, the detergent-depleted phase was found to contain AMs, while the detergent-rich phase included lipoglycans identified as ManLAMs and LMs. To remove the LMs from the ManLAMs, the corresponding cellular and parietal fractions were purified by Bio-Gel P-100 gel filtration in the presence of sodium deoxycholate buffer.

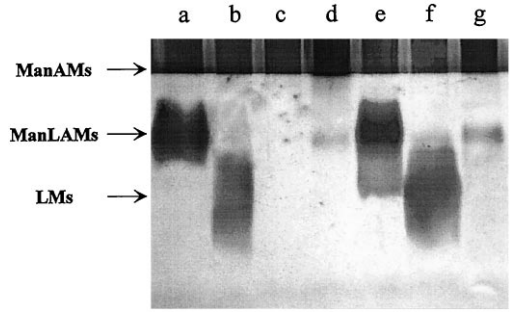

FIG. 3. **SDS-PAGE analysis of parietal and cellular ManLAMs and related mannoconjugates from *M. bovis* BCG Pasteur strain.** 20 μg of parietal ManLAMs (*lane a*), 20 μg of parietal LMs (*lane b*), 20 μg of parietal ManAMs (*lane c*), 200 μg of parietal ManAMs (*lane d*), 20 μg of cellular ManLAMs (*lane e*), 20 μg of cellular LMs (*lane f*), 200 μg of cellular ManAMs (*lane g*). The gel was colored with a silver stain containing periodic acid.

Both fractions gave a similar chromatographic profile (Fig. 2) characterized by two peaks, I and II. From SDS-PAGE analysis, peak I was assigned to the ManLAMs, while peak II corresponded to LMs. Moreover, whatever their parietal or cellular origin, ManLAMs and LMs showed the same electrophoretic behavior on SDS-PAGE (Fig. 3). These assignments are in agreement with routine carbohydrate analysis, which showed that parietal and cellular ManLAMs contained, besides inositol, arabinose and mannose in a ratio of 1.4 and 1.6, respectively. Likewise, mannose and inositol were both found in the cellular and parietal LMs fractions.

Purification scheme (Fig. 1) summarizes the amounts of ManLAMs, LMs, and ManAMs[2] of either parietal or cellular origin recovered by our procedure. It can be observed that the total amount of cellular material obtained (492 mg) was much higher than for parietal material (93 mg). Moreover, it must be underlined that the cellular ManLAMs were twice as abundant as the cellular ManAMs, whereas the parietal ManLAMs were only half as abundant as the parietal ManAMs.

Structural Features of Parietal and Cellular ManLAMs

As indicated in the literature, fatty acid residues (5, 8) and mannooligosaccharide caps (9, 10) seem to be the key structural features determining the ManLAM immunological activ-

[2] Parietal and cellular AMs were identified as ManAMs, *i.e.* with mannosyl extensions on the arabinan side chains (J. Nigou, M. Gilleron, and G. Puzo, unpublished observation).

TABLE I
Methylation analysis data of parietal and cellular ManLAMs from M. bovis BCG Pasteur strain
Molar ratio values are corrected by the use of effective carbon-response factors (26).

	Abbreviated name of the glycosyl residue	Parietal ManLAMs	Cellular ManLAMs
		mol %	
Partially methylated alditols acetates			
2,3,5-Tri-*O*-Me-1,4-di-*O*-Ac-arabinitol	t-Ara*f*	2.3	5.6
3,5-Di-*O*-Me-1,2,4-tri-*O*-Ac-arabinitol	2-*O*-Linked Ara*f*	7.5	7.4
2,3-Di-*O*-Me-1,4,5-tri-*O*-Ac-arabinitol	5-*O*-Linked Ara*f*	38.3	35.6
2-*O*-Me-1,3,4,5-tetra-*O*-Ac-arabinitol	3,5-Di-*O*-linked Ara*f*	9.8	10.7
2,3,4,6-Tetra-*O*-Me-1,5-di-*O*-Ac-mannitol	t-Man*p*	23.4	17.7
3,4,6-Tri-*O*-Me-1,2,5-tri-*O*-Ac-mannitol	2-*O*-Linked Man*p*	9.2	9.4
2,3,4-Tri-*O*-Me-1,5,6-tri-*O*-Ac-mannitol	6-*O*-Linked Man*p*	2.7	5.3
3,4-Di-*O*-Me-1,2,5,6-tetra-*O*-Ac-mannitol	2,6-Di-*O*-linked Man*p*	6.8	8.3
Mancapping percentage			
[a]		76	48
[b]		69	24

[a] 3,5-Di-*O*-linked Ara*f* − t-Ara*f* to 3,5-di-*O*-linked Ara*f* ratio.
[b] 2-*O*-Linked Ara*f* − t-Ara*f* to 2-*O*-linked Ara*f* ratio.

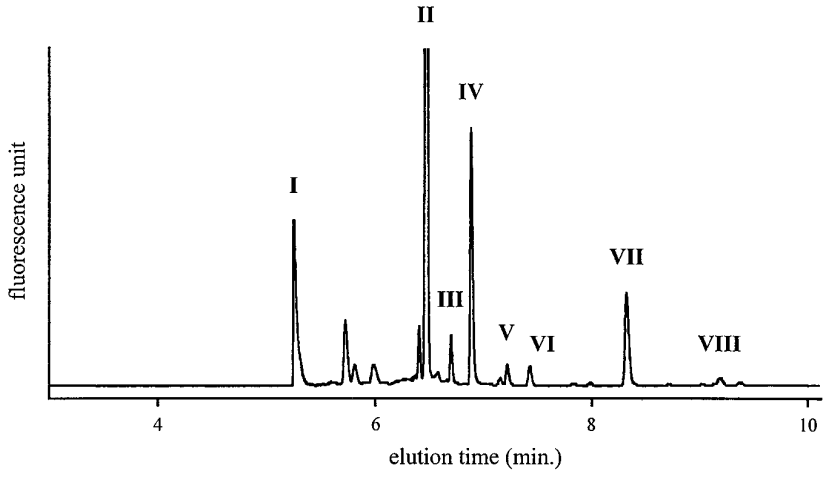

FIG. 4. **Electrophoregram of oligosaccharides derivatives obtained from the parietal ManLAMs after mild hydrolysis (0.1 N HCl, 30 min at 110 °C) and derivatization with APTS.** 1.3 ng of oligosaccharide-APTS derivatives were loaded on a 470 mm × 50-μm capillary. Analysis was carried out at a temperature of 20 °C with an applied voltage of 24 kV and monitored by laser-induced fluorescence. *Peak I*, APTS; *peak II*, Ara-APTS; *peak III*, Man-APTS; *peak IV*, mannoheptose-APTS reference; *peak V*, Ara*f*-Ara-APTS; *peak VI*, Man*p*-Ara-APTS; peak VII, Man*p*-Man*p*-Ara-APTS; peak VIII, Man*p*-Man*p*-Man*p*-Ara-APTS.

ity. We therefore investigated the presence and structure of the fatty acids and mannooligosaccharide caps in parietal and cellular ManLAMs.

Mannooligosaccharide Caps—To characterize the expected mannooligosaccharide caps, parietal and cellular ManLAMs were analyzed by ^{1}H-^{13}C HMQC experiments (data not shown) as described previously by Venisse *et al.* (11). The parietal ManLAM C-1 resonances at δ 104.7 and δ 100.8 were respectively assigned to 2-*O*-linked α-Man*p*s and t-α-Man*p*s. Each of these resonances correlate with two different proton resonances at δ 5.14, δ 5.12 and δ 5.06, δ 5.04, respectively, in agreement with the presence of (1→2)-α-D-mannooligosaccharide caps. Likewise, these mannooligosaccharide caps were found in the cellular ManLAMs. These cap structures were also supported by the identification of 2-*O*-linked Man*p*s from the alditol acetate analysis of the parietal and cellular ManLAMs (Table I). From these data, the capping percentage was determined from the (3,5-di-*O*-linked Ara*f* − t-Ara*f*) to (3,5-di-*O*-linked Ara*f*) ratio. It was found that the capping frequency of the parietal ManLAMs (76%) was higher compared with that of the cellular ManLAMs (48%). The structures of these mannooligosaccharide caps were then investigated by capillary electrophoresis analysis. Both parietal and cellular ManLAMs were submitted to mild acid hydrolysis, to APTS tagging followed by reductive amination (21), and finally, the oligosaccharides derivates were analyzed by capillary electrophoresis monitored by laser-induced fluorescence. Fig. 4 represents the electrophoregram of the APTS derivatives arising from the parietal ManLAMs showing eight peaks assigned by coelectrophoresis using oligosaccharide-APTS standards and by previous data on the parietal ManLAM mannooligosaccharide structures (11). Peak I was assigned to free APTS reagent; peak II, which corresponds to the major compound, was Ara-APTS; peak III, Man-APTS; peak IV, mannoheptose-APTS reference; peak V, Ara*f*-Ara-APTS; peak VI, Man*p*-Ara-APTS; peak VII, Man*p*-Man*p*-Ara-APTS; and finally peak VIII, Man*p*-Man*p*-Man*p*-Ara-APTS. The relative quantitation of the different mannooligosaccharide caps was achieved by peak integration (21). The major structural motif was the dimannosyl unit (78%), while mannosyl (15%) and trimannosyl (7%) were less frequent. Likewise, it was established that cellular ManLAMs contained the same mannooligosaccharide cap structures and in similar amounts to parietal ManLAMs, *i.e.* 76, 17, and 7%, respectively.

In summary, parietal and cellular ManLAMs share the same mannooligosaccharide cap structure but differ in their capping frequency, which was 76 and 48%, respectively.

Phosphatidyl-myo-inositol Anchor—Both parietal and cellular ManLAMs were found to contain phosphorus and *myo*-inositol, which are parts of the PI anchor. It was established by routine GC that cellular ManLAMs contained 2.3 palmitic and 1.0 tuberculostearic acids/phosphorus atom. Surprisingly, these fatty acids were not observed in significant amounts in parietal ManLAMs. So, the PI anchor structure of parietal ManLAMs was investigated by two-dimensional heteronuclear NMR techniques.

The one-dimensional ^{31}P spectrum of parietal ManLAMs showed a single resonance at −0.066 ppm attributed to the phosphodiester from the anchor (Fig. 5*a*). By means of the

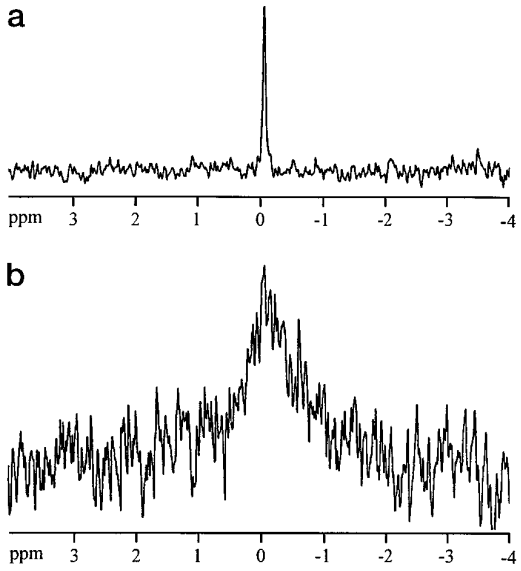

FIG. 5. **One-dimensional ^{31}P NMR spectrum (δ^{31}P: −4.00 to 4.00) of the parietal (*a*) and cellular (*b*) ManLAMs from *M. bovis* BCG Pasteur strain.** The spectra were recorded in D_2O at 313 K.

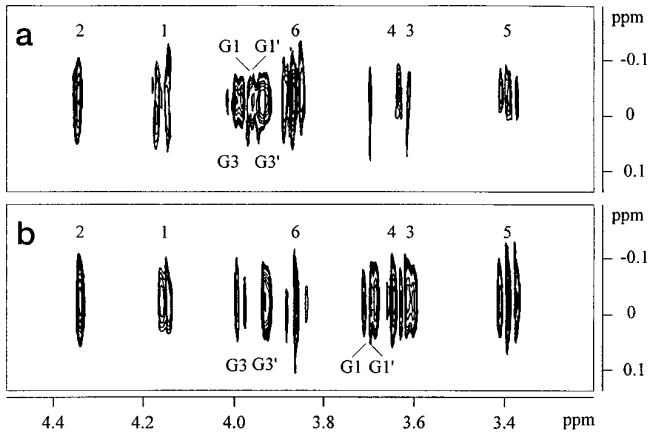

FIG. 6. **Expanded region (δ^1H: 3.20–4.50; ^{31}P: −0.20 to 0.15) of the ^{31}P-decoupled, ^{1}H-detected HMQC-HOHAHA spectrum of the native (*a*) and deacylated (*b*) parietal ManLAMs.** Numerals correspond to the proton number of the *myo*-inositol units and numerals with letter *G*, to the proton number of the glycerol units.

^{1}H-^{31}P HMQC and HMQC-HOHAHA experiments, the proton resonances of the residues esterifying the phosphorus were assigned. The ^{1}H-^{31}P HMQC spectrum (data not shown) showed three direct correlations between phosphate and proton resonances at δ 4.16, 3.99, and 3.93 tentatively assigned by analogy to the literature data (15) to the H-1 of the *myo*-inositol and H-3 and H-3′ of the glycerol, respectively. The *myo*-inositol was typified by the ^{1}H-^{31}P HMQC-HOHAHA spectrum (Fig. 6*a*) showing resonances at δ 4.34, 4.16, 3.87, 3.65, 3.61, and 3.40 respectively assigned to H-2, H-1, H-6, H-4, H-3, and H-5 of *myo*-inositol from the HOHAHA experiments (data not shown) and literature data (15). The downfield resonances of H-2 (Δδ +0.11) and H-6 (Δδ +0.13) are in agreement with the expected anchor structure characterized by a glycosylation of the *myo*-inositol at C-6 by the mannan core and at C-2 by one Man*p* unit. From the ^{1}H-^{31}P HMQC-HOHAHA spectrum, it was deduced that the remaining glycerol proton H-1, H-1′, and H-2 resonances overlapped between δ 3.99 and δ 3.93, revealing that only the C-1 position is acylated thanks to the following literature data: 1,2-diacyl-3-phospho-*sn*-glycerol unit ($\delta_{H\text{-}1/H\text{-}1'}$ 4.25/4.03; $\delta_{H\text{-}2}$ 5.12) (27); 3-phosphoglycerol unit, ($\delta_{H\text{-}1/H\text{-}1'}$ 3.68/3.61; $\delta_{H\text{-}2}$ 3.90) (28). Moreover, the H-1 and H-1′ resonance upfield shift (Δδ = 0.26 to 0.1 ppm) is in agreement with the absence of an acyl substituent on C-2. Thus, a lyso structure can be proposed for the parietal ManLAM phosphatidyl moiety.

To support this lyso structure, the parietal ManLAMs were treated under mild alkaline conditions followed by their analysis by one-dimensional ^{31}P and two-dimensional ^{1}H-^{31}P HMQC (not shown) and HMQC-HOHAHA experiments (Fig. 6*b*). As expected, the glycerol H-3 and H-3′ resonate at the same values as those described for the native parietal ManLAMs, *i.e.* δ 3.99 and 3. 93. However, the H-1 and H-1′ are shifted upfield to δ 3.71 and δ 3.68 (Δδ = 0.25 ppm, approximately) in agreement with the C-1 deacylation of the glycerol moiety. H-2 still overlaps with H-3 and H-3′ precluding its precise localization, but confirming that this position is not acylated. Taken together, these data demonstrate that the parietal ManLAM PI anchor differs from the cellular one and from those previously described in the literature by the absence of C_{16} and C_{19} fatty acids and by the presence of an unidentified acyl residue borne by the C-1 of the glycerol unit.

This two-dimensional ^{1}H-^{31}P NMR analytical approach, which allowed the structural elucidation of the phosphate substituents, could not be applied to the native cellular ManLAMs. In contrast to the parietal ManLAMs, which showed a sharp peak in the one-dimensional ^{31}P spectrum (with a width of 9 Hz), the cellular ManLAM spectrum exhibited a broad unresolved signal centered at 0 ppm with a width of 150 Hz (Fig. 5*b*). In this case, no connectivities between phosphate and protons were obtained in the two-dimensional ^{1}H-^{31}P HMQC and HMQC-HOHAHA experiments. This phenomenon was systematically observed when phosphorus did not resonate as a well resolved sharp signal, indicating a restricted mobility of the phosphate groups possibly due to aggregation of the cellular ManLAMs as a consequence of their amphipathic nature (29). Indeed, the deacylated cellular ManLAMs showed a sharp phosphate resonance signal allowing the two-dimensional ^{1}H-^{31}P NMR approach to be applied. An expected structure of the PI anchor was found, in which the *myo*-inositol was esterified at C-1 by the phosphate and glycosylated at C-2 by one α-D-Man*p* unit and at C-6 by the mannan core. In conclusion, the NMR study indicates that the parietal and cellular ManLAMs also differ through the lipid part of the PI anchor.

To determine the structure of the acyl group borne by the glycerol moiety of the parietal ManLAMs and also to define the PI anchor structure of the cellular ManLAMs, a new analytical procedure was developed. ManLAMs were submitted to acetolysis allowing cleavage between phosphate and glycerol, but preserving the acyl-glycerol residues (20). These residues, extracted by cyclohexane/water partition, were analyzed by GC/MS in EI and CI/NH_3 ionization modes. The cellular ManLAMs EI-total ion current chromatogram profile (Fig. 7*a*) shows five peaks of interest. Four of them were assigned from the EI and CI mass spectra analysis. Peak I is attributed either to 1- or 2-palmitoyldiacetyl-*sn*-glycerol from the CI spectrum dominated by the $(M + NH_4)^+$ ions at *m/z* 432 and the EI fragment ions at *m/z* 354 $(M\text{-}CH_3COOH)^{+\bullet}$; *m/z* 239 $CH_3\text{-}(CH_2)_{14}\text{-}C{\equiv}O^+$ and *m/z* 159 $(M\text{-}CH_3\text{-}(CH_2)_{14}\text{-}COO^{\bullet})^+$. Likewise peak II is assigned to either 1- or 2-tuberculostearoyldiacetyl-*sn*-glycerol. Finally, peaks IV and V are assigned to 1,2-dipalmitoyl-3-acetyl-*sn*-glycerol and 1-tuberculostearoyl-2-palmitoyl-3-acetyl-*sn*-glycerol, respectively. In the last compound, the palmitoyl residue was unequivocally localized at the C-2 position from the reporter ion *m/z* 341 arising from the fragmentation of the molecular ions between C-1 and C-2 of glycerol resulting in charged fragments having lost the primary ester group together with C-1 (30). These data reveal the het-

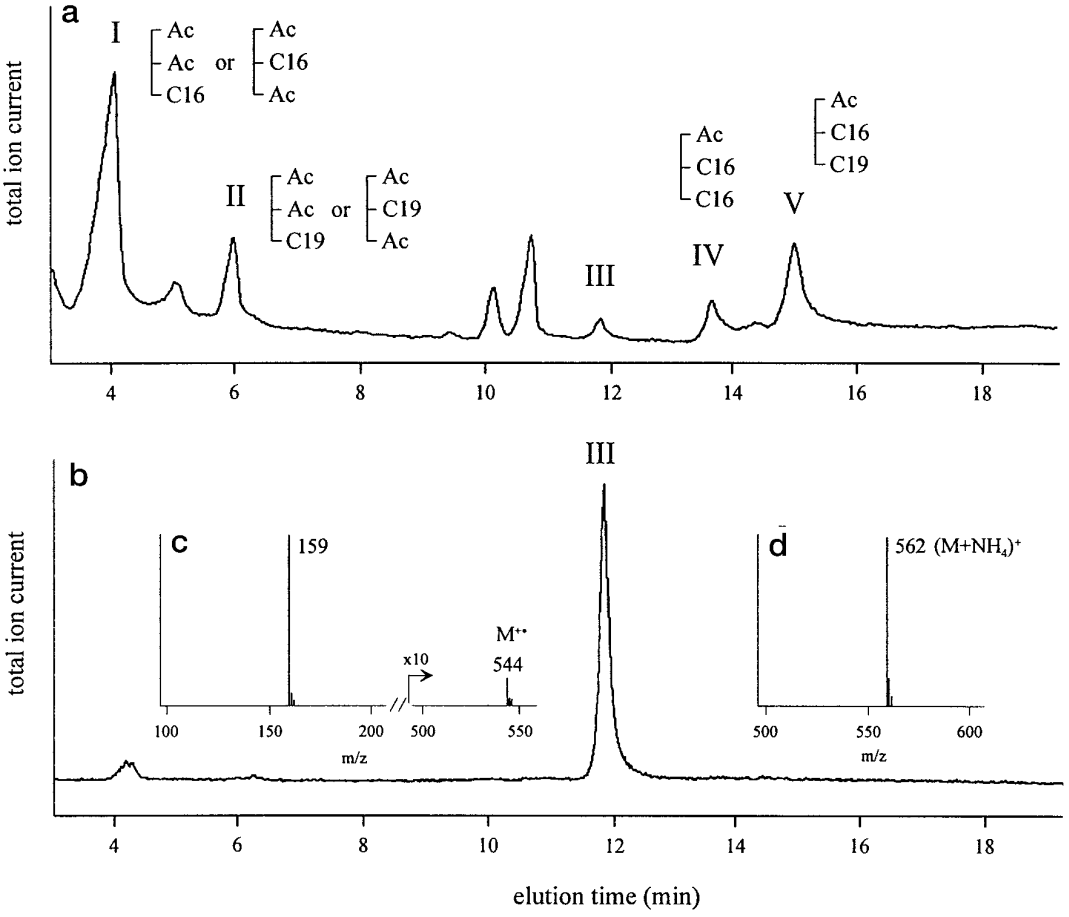

FIG. 7. **GC/MS chromatogram profile in EI mode of the acetolysis subproducts from cellular (*a*) and parietal (*b*) ManLAMs.** *Peak I* was assigned to 1-palmitoyl-2,3-diacetyl-*sn*-glycerol or to 1,3-diacetyl-2-palmitoyl-*sn*-glycerol according to following ions, in CI mode m/z 432 $(M + NH_4)^+$, in EI mode m/z 354 $(M\text{-}CH_3COOH)^{+\bullet}$, 239 $(C_{15}H_{31}CO)^+$, 159 $(M\text{-}C_{15}H_{31}COO^{\bullet})^+$. Likewise, *peak II* was assigned to 1-tuberculostearoyl-2,3-diacetyl-*sn*-glycerol or to 1,3-diacetyl-2-tuberculostearoyl-*sn*-glycerol according to m/z 474 $(M + NH_4)^+$ in CI mode, m/z 396 $(M\text{-}CH_3COOH)^{+\bullet}$, 281 $(C_{18}H_{37}CO)^+$, 159 $(M\text{-}C_{18}H_{37}COO^{\bullet})^+$ in EI mode. *Peak IV* was assigned to 1,2-dipalmitoyl-3-acetyl-*sn*-glycerol, m/z 628 $(M + NH_4)^+$ in CI mode, m/z 550 $(M\text{-}CH_3COOH)^{+\bullet}$, 355 $(M\text{-}C_{15}H_{31}COO^{\bullet})^+$, 341 $(M\text{-}^{\bullet}CH_2OCOC_{15}H_{31})^+$, 313 $(M\text{-}C_{15}H_{31}COO^{\bullet}\text{-}CH_2CO)^+$, 239 $(C_{15}H_{31}CO)^+$ in EI mode. *Peak V* was assigned to 1-tuberculostearoyl-2-palmitoyl-3-acetyl-*sn*-glycerol, m/z 670 $(M + NH_4)^+$ in CI mode, m/z 592 $(M\text{-}CH_3COOH)^{+\bullet}$, 397 $(M\text{-}C_{15}H_{31}COO^{\bullet})^+$, 355 $(M\text{-}C_{18}H_{37}COO^{\bullet})^+$, and $(M\text{-}C_{15}H_{31}COO^{\bullet}\text{-}CH_2CO)^+$, 341 $(M\text{-}^{\bullet}CH_2OCOC_{18}H_{37})^+$, 313 $(M\text{-}C_{18}H_{37}COO^{\bullet}\text{-}CH_2CO)^+$, 281 $(C_{18}H_{37}CO)^+$, 239 $(C_{15}H_{31}CO)^+$ in EI mode. *c*, EI spectrum of compound III; *d*, CI/NH_3 spectrum of compound III. Unnumbered peaks (in *a*) correspond to contaminants. *Ac*, C_{16}, and C_{19} represent acetyl, palmitoyl, and tuberculostearoyl residues esterifying glycerol.

erogeneity of the phosphatidyl moiety, since at least four molecular species were identified that differ in C_{16} and C_{19} fatty acid composition and location. From the integration of the total ion current chromatogram peaks, corrected by a response factor, compound V is the major component (53%), while compound II is the least abundant (5%). Finally, compounds I and IV represent 22 and 19, respectively. Due to its low abundance (1%), compound III could not be identified.

The parietal ManLAM EI-total ion current chromatogram profile (Fig. 7*b*) shows only one peak with a retention time corresponding to the unidentified compound III from the cellular ManLAMs. The EI spectrum (Fig. 7*c*) is dominated by the fragment ions at m/z 159 typifying a lyso-glycerol and, in the high mass range, by the peak at m/z 544 tentatively assigned to the molecular ions. Indeed, the CI/NH_3 spectrum (Fig. 7*d*) shows one peak located at the expected value of m/z 562 $(M + NH_4)^+$ confirming the molecular weight of 544 Da. From this latter value, a molecular weight of 386 Da was deduced for the fatty acid, suggesting the presence of two oxygen atoms tentatively assigned to two hydroxyl groups. This hypothesis is supported by the fact that these fatty acids were not detected by routine GC analysis. Therefore, the fatty acids released by alkaline hydrolysis of parietal ManLAMs were derivatized as methyl esters, peracetylated, and analyzed by GC and GC/MS in EI and CI/NH_3 ionization modes. The GC chromatogram (not shown) is dominated by one peak attributed to a fatty acid methyl ester of 356 Da molecular mass, containing one acetyl group instead of two as previously expected, consistent with a monohydroxyl stearic acid. However, the molecular mass of the acetylated fatty acid (342 Da) is 44 mass units lower than the one expected. To support this conclusion and to localize the hydroxyl function, the fatty acid methyl esters obtained from parietal ManLAMs were trimethylsilylated and analyzed by GC/MS. The chromatogram (Fig. 8*a*) is dominated by one peak (*peak 4*) assigned to a TMS fatty acid methyl ester of 386 Da molecular mass (Fig. 8*b*). This is in agreement with the mass difference of 30 Da between a TMS and an acetyl residue and confirms a monohydroxyl stearic acid structure. Moreover, from the reporter EI-fragment ions at m/z 187 and 301 (Fig. 8*c*), this hydroxyl group was unambiguously localized at C-12.

In summary, TMS and peracetylation analysis converge to a 12-hydroxystearic acid structure, but with a molecular mass of 300 Da, which is 86 Da lower than that deduced from the acetolysis-GC/MS experiments. Thus, it is tempting to conclude that the hydroxyl function in the native parietal ManLAMs was not free, but rather esterified by a methoxypropanoic residue. Besides this major fatty acid (Fig. 8*a*), palmitic acid, stearic acid, and a 12-hydroxytuberculostearic acid were found

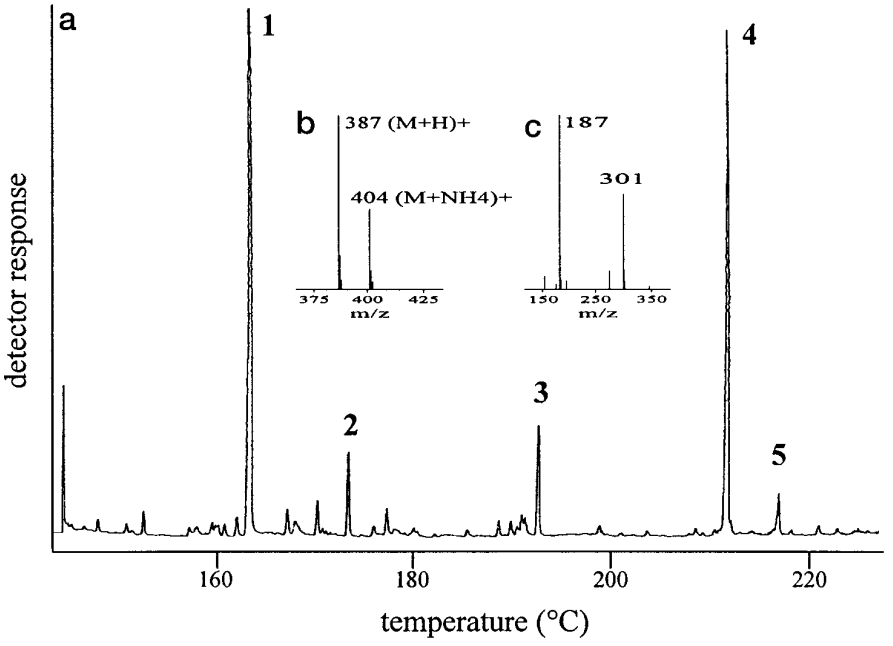

FIG. 8 *a*, flame ionization detector gas chromatogram profile of the trimethylsilylated fatty acid methyl esters from parietal ManLAMs. *Peak 1*, C_{15} methyl ester reference; *peak 2*, C_{16} methyl ester; *peak 3*, C_{18} methyl ester; *peak 4*, 12-*O*-TMS-12-hydroxystearic acid methyl ester assigned according the following ions, in CI/NH_3 mode (*b*) *m/z* 387 $(M + H)^+$, 404 $(M + NH_4)^+$, in EI mode (*c*) *m/z* 187 $(CH_3\text{-}(CH_2)_5CH = O^+Si(CH_3)_3)$, 301 $((CH_3)_3SiO^+ = CH(CH_2)_{10}CO_2CH_3)$; *peak 5*, 12-*O*-TMS-12-hydroxytuberculostearic acid methyl ester assigned according the following ions, in CI mode *m/z* 401 $(M + H)^+$, 418 $(M + NH_4)^+$, in EI mode *m/z* 187 and 315 and the reporting ions at *m/z* 149 and 167 typifying a C-methyl ramification located at position 10 (31).

in small amounts as their methyl ester derivatives: *peaks 2, 3*, and *5*, respectively.

Secretion of IL-8 and TNF-α by Human DCs in Response to Parietal and Cellular ManLAMs

To investigate the consequences of the structural differences established between parietal and cellular ManLAMs on their immunological activity, we compared the ability of parietal and cellular ManLAMs to stimulate cytokine release from human DCs. DCs are the most professional antigen-presenting cells specifically adapted to initiate T cell responses. In addition to this function, DCs are capable of producing a number of cytokines, including chemokines that recruit other leukocytes to the sites of antigen contact. It is now well established that DCs differentiate from human monocytes in the presence of IL-4 and GM-CSF (32). Using this system, we have shown previously that BCG is a potent stimulus for DCs (25). BCG induces a maturational step in DCs that is accompanied by the up-regulation of surface markers such as CD83 and CD86 and by the down-regulation of the endocytic activity. In addition, BCG induces the release of TNF-α and IL-8[3] from DCs.

In the present work we compared the ability of parietal and cellular ManLAMs to stimulate the production of IL-8 in DCs. Fig. 9*a* demonstrates that parietal ManLAMs induce IL-8 secretion in a dose-dependent manner. Unstimulated DCs produced low basal levels of IL-8 ranging from 50 to 150 pg/ml/10^5 cells. Parietal ManLAMs at a dose of 10 μg/ml stimulated IL-8 release more than 25-fold. In contrast, cellular ManLAMs exhibited significantly less stimulatory activity. The IL-8 stimulatory activity was completely abolished after removal of the fatty acid residues by mild alkaline treatment. Moreover, ManAMs that lack the PI anchor failed to release significant amounts of IL-8 when used at the same concentration (data not shown).

Previous works have shown that ManLAMs from *M. tuberculosis* Erdman are poor inducers of TNF-α release from the THP-1 monocytic cell line compared with the PI-GAMs from *M. smegmatis*, which correspond to the parietal LAMs (5, 7). We therefore investigated the effect of the two types of ManLAMs on TNF-α production by DCs. Parietal ManLAMs at 10 μg/ml

[3] M. Thurnher, unpublished data.

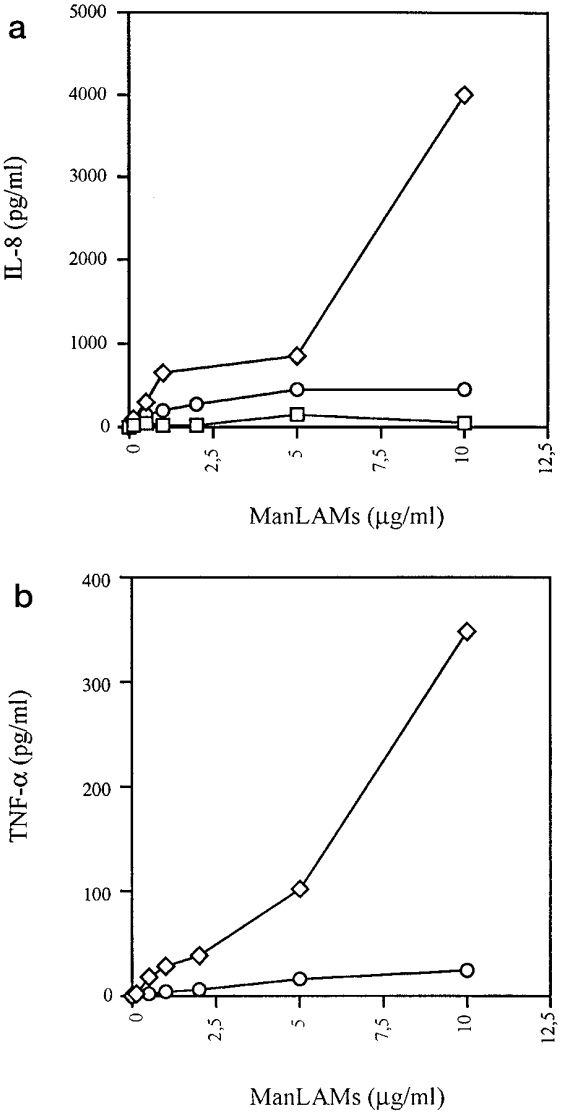

FIG. 9. **IL-8 (*a*) and TNF-α (*b*) release by human dendritic cells stimulated by parietal ManLAMs (◇), cellular ManLAMs (○), and deacylated cellular ManLAMs (□).**

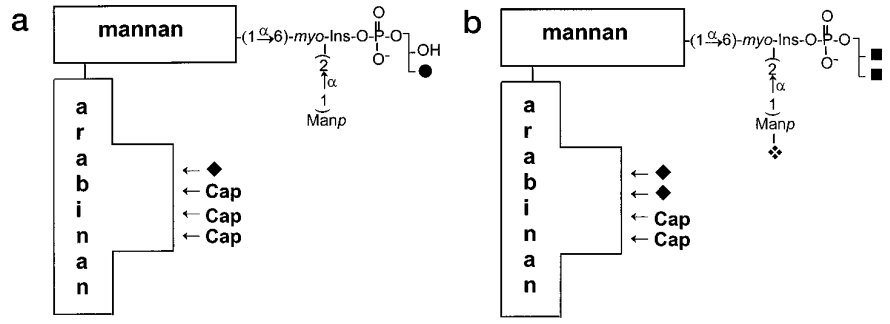

FIG. 10. **Partial structural models proposed for the parietal (*a*) and the cellular (*b*) ManLAMs from *M. bovis* BCG Pasteur strain.** ●, 12-*O*-(methoxypropanoyl)-12-hydroxystearic acid; ■,■ represents at 53% C_{19}, C_{16}; at 22% OH, C_{16}; at 19% C_{16}, C_{16}; at 5% OH, C_{19}; at 1% OH, 12-*O*-(methoxypropanoyl)-12-hydroxystearic acid; ❖, fatty acid or not; ◆, t-β-Ara*f*; **Cap** corresponds to 77% dimannosyl unit, 16% mannosyl unit, and 7% trimannosyl unit. The percentage of capping is 76 and 48% for the parietal and cellular ManLAMs, respectively.

induced the secretion of more than 300 pg/ml TNF-α, while cellular ManLAMs at the same concentration almost failed to elicit TNF-α secretion (Fig. 9*b*). This finding is consistent with a previous report demonstrating that cellular ManLAMs were unable to induce TNF-α from THP-1 cells (7).

DISCUSSION

LAMs are important mycobacterial antigens that can be recognized by T cells in the context of CD1 molecules. However, CD1-restricted T cell lines were shown to discriminate between ManLAMs derived from *M. leprae* and *M. tuberculosis*, suggesting subtle but significant structural differences which can, up to date, only be explained by differences in the mannooligosaccharide cap frequency (10). This assumption was also recently advanced by Schlesinger *et al*. (33) to explain differences in the ability of ManLAMs from Erdman and H37Ra to serve as ligands for the macrophage mannose receptors. In addition, LAMs can stimulate the production of cytokines such as TNF-α in monocytes/macrophages, thereby contributing to the clearance of mycobacteria. Conversely, it has been suggested that the poor cytokine stimulatory activity of LAMs from virulent mycobacteria is responsible for the intramacrophagic persistence of the mycobacteria (5). However, the molecular basis underlying these differences in the immunological activity of LAMs are poorly understood. Thus, despite continuing efforts of Brennan's and Puzo's groups to establish detailed structures of ManLAMs based on the use of sophisticated analytical tools such as two-dimensional NMR spectroscopy and matrix-assisted laser desorption/ionization mass spectrometry, the above mentioned immunological LAM properties suggest that the present structural models are incomplete. This paradoxical situation can be explained by the structural complexity of the ManLAMs, but also and essentially by the molecular heterogeneity of the ManLAM fractions analyzed. So, it appears clearly that the obtention of homogenous ManLAM fractions remains a key step in the understanding, at the molecular level, of the ManLAM properties. Analyses of ManLAMs by matrix-assisted laser desorption/ionization mass spectrometry revealed substantial molecular weight heterogeneity estimated to be 6 kDa and attributed to differences in the degree of glycosylation of the mannan core and the arabinan domain. More detailed structural studies of the parietal ManLAMs from *M. bovis* BCG revealed two equally frequent types of mannan core, which differ at their reducing end by the presence or absence of the phosphatidyl-*myo*-inositol anchor, but also by the t-Man*p*-(α1→2)-Man*p* branching frequency, suggesting that the parietal ManLAM preparation was contaminated by ManAMs (15).

In this report, we present a new extraction and purification protocol for ManLAMs from BCG. According to its extraction mode two types of ManLAMs were distinguished and designated as parietal and cellular (16). The parietal ManLAMs were obtained, as described by Venisse *et al.* (11), from extraction of delipidated cells by an ethanol/water mixture, while the cellular ManLAMs were obtained from the resulting cells disrupted and extracted as mentioned above. The second major feature of this new protocol was the fractionation of the ManAMs and ManLAMs using the Triton X-114 phase separation method. This approach was previously applied to completely resolve membranous lipopolysaccharides and membranous proteins of *M. leprae* (34) or to remove LPS from exopolysaccharides (35). ManLAMs are amphipathic molecules that aggregate with ManAMs, hindering their separation either by anion exchange or gel filtration chromatography. Triton X-114 improves the dissociation of amphipathic and hydrophilic molecules and, at temperatures beyond the cloud point (22 °C), the detergent-rich phase was found, by SDS-PAGE, to contain the ManLAMs, while the ManAMs were present in the detergent-depleted phase. Thus, the Triton X-114 partitioning method appears to be a powerful approach to efficiently remove ManAMs from the ManLAMs. So, ManLAMs devoid of ManAMs were obtained and two types of ManLAMs, called parietal and cellular, were structurally defined for *M. bovis* BCG. Quantitative analysis of the individual fractions revealed that parietal mannoconjugates were less abundant than cellular ones, 16 and 84%, respectively, and that the proportion of cellular ManLAMs was 10 times higher than the parietal ManLAMs.

The comparative structural analysis of the two ManLAMs revealed subtle structural differences between the parietal and cellular ManLAMs (Fig. 10), supporting the pertinence of the extraction and purification strategy. Structural differences include the percentage of the mannooligosaccharide caps and the PI anchor lipid moiety. Capping is more frequent in the parietal ManLAMs (76%) as compared with cellular ones (48%). These values were determined from the (3,5-di-*O*-linked Ara*f* − t-Ara*f*) to 3,5-di-*O*-linked Ara*f* unit ratio established routinely from the alditol acetates analysis. Alternatively, it can also be calculated from the (t-Man*p* − 2,6-di-*O*-linked Man*p*) to 3,5-di-*O*-linked Ara*f* ratio, but in this case the percentage of t-Man*p* caps is higher (16.6%) than the percentage of 3,5-di-*O*-linked Ara*f* (9.8%). This observation can be explained by the low amount of di-*O*-linked Man*p* compared with t-Man*p* released during hydrolysis of the ManLAMs (36). Another method has been used as the (2-Ara*f* − t-Ara*f*) to 2-Ara*f* ratio (36), leading to capping frequencies of 69 and 24% for the parietal and cellular ManLAMs, respectively (Table I). However this approach may be less accurate, since it is based on the assumption that each arabinan side chain contains only one 2-*O*-linked Ara*f* unit. Nevertheless, whatever the method applied, the capping of parietal ManLAMs is more frequent than capping of cellular ManLAMs. The ManLAM mannooligosaccharide cap structures were previously described as single α-Man*p*, Man*p*-(1α→2)-Man*p* and Man*p*-(1α→2)-Man*p*-(1α→2)-Man*p* using LC/MS (11). A new analytical approach, based on mild hydrolysis of ManLAMs, tagging by APTS followed by capillary electrophoresis analysis monitored by laser-induced fluorescence, was applied to both parietal and cellular ManLAMs. The same three structures of mannooligosaccharide caps were evidenced with the same relative abundance for both parietal and cellular

ManLAMs: α-Man*p* (16 ± 1%), Man*p*-(1α→2)-Man*p* (77 ± 1%), and Man*p*-(1α→2)-Man*p*-(1α→2)-Man*p* (7 ± 1%). Relative quantification was achieved by peak integration. The analysis was performed in the microgram range of ManLAMs, demonstrating the sensitivity of this method.

The other unexpected difference between parietal and cellular ManLAMs concerned the lipid part of the ManLAM PI anchors. The cellular ManLAM anchors were mainly found to contain 1- or 2-palmitoyl-*sn*-glycerol (22%), 1- or 2-tuberculostearoyl-*sn*-glycerol (5%), 1,2-dipalmitoyl-*sn*-glycerol (19%), and 1-tuberculostearoyl-2-palmitoyl-*sn*-glycerol (53%). In contrast, the parietal ManLAM PI anchor was found to be composed of a single type of acylglycerol identified as the unusual 1-[12-*O*-(methoxypropanoyl)-12-hydroxystearoyl]-*sn*-glycerol.

Finally, we were interested in the biological effects of these structurally different ManLAMs from BCG. Both parietal and cellular ManLAMs of BCG induced expression of IL-8 and TNF-α from human DCs. However, parietal ManLAMs turned out to be better stimulators of IL-8 production in DCs compared with cellular ManLAMs. It was previously reported that H37Ra and its LAMs were able to stimulate the release of IL-8 from human alveolar macrophages, although the identification of the mycobacterial species remains suspicious (37). In addition, we found that only parietal ManLAMs stimulated TNF-α secretion from DCs. This last point is consistent with our earlier finding that cellular ManLAMs are unable to stimulate TNF-α secretion from THP-1 cells (7). It thus appears that structural modifications of ManLAMs are able to regulate expression of the cytokines involved in macrophage and dendritic cell activation. Structural differences between cellular and parietal ManLAMs affect the percentage of mannooligosaccharide caps and the lipid part of the PI anchor. The fact that the ManLAM activities are abrogated after deacylation and the observation that ManAMs, which lack the PI anchor, are unable to stimulate cytokine production are consistent with the assumption that the PI anchor lipid part is an essential element for the immunological activities of the ManLAMs.

The parietal ManLAM PI anchor lipid part is characterized by the presence of a unique fatty acid, found for the first time in the mycobacteria genus and identified as 12-*O*-(methoxypropanoyl)-12-hydroxystearic acid. Moreover, this fatty acid was found to exclusively acylate the glycerol at C-1 leading to a lyso form. Therefore, it is intriguing to speculate that this acylglycerol modification could regulate cytokine secretion and consequently modulate intracellular survival of mycobacteria. Indeed, it was recently established that LPS from *Salmonella typhimurium*, modified by the addition of a hydroxymyristate in the lipid A part, altered TNF-α expression by adherent cells (38). More excitingly, it was found that these modifications were under the control of virulence genes (*phoP-phoQ*). It can be advanced that mycobacteria can escape from intramacrophagic destruction by adapting their ManLAM PI anchor structures to prevent stimulation of cytokine synthesis. Further structural definition of anchors from pathogenic mycobacteria species will help to clarify their role in mycobacterial virulence. As reported previously, ManLAMs are also ligands of the mannose receptor expressed on macrophages and DCs. ManLAMs thus favor mycobacterial adhesion. Concomitantly, however, ManLAMs internalized via mannose-receptor-mediated endocytosis can be presented in the context of CD1 and stimulate antimycobacterial T cell responses. It should also be considered that structural differences may affect uptake, intracellular handling, and cell surface presentation of individual ManLAM molecules. Besides the PI anchor, it was found that the mannooligosaccharide caps play a key role in the adhesion to macrophages and the subsequent induction of T-lymphocyte responses, suggesting that the molecular basis of ManLAM functional diversity is not yet precisely understood.

To further clarify these molecular mechanisms of recognition, it will be important, in future studies, to establish detailed structures of parietal and cellular ManLAMs from virulent and pathogenic mycobacterial strains and to compare their activities in biological processes such as cell adhesion, antigen presentation, cytokine stimulation, and T cell activation.

Acknowledgments–We gratefully acknowledge Dr. Alain Vercellone and Dr. Olivier Adam for stimulating discussions and Therese Brando and Christine Papesh for technical assistance.

REFERENCES

1. Bloom, B. R., and Murray, G. J. (1992) *Science* **257,** 1055–1064
2. Fine, P. E. M. (1989) *Rev. Infect. Dis.* **11,** S353–S359
3. Roche, P. W., Triccas, J. A., and Winter, N. (1995) *Trends Microbiol.* **3,** 397–401
4. Britton, W. J., Roche, P. W., and Winter, N. (1994) *Trends Microbiol.* **2,** 284–288
5. Roach, T. I. A., Barton, C. H., Chatterjee, D., and Blackwell, J. M. (1993) *J. Immunol.* **150,** 1886–1896
6. Chan, J., Fan, X., Hunter, S. W., Brennan, P. J., and Bloom, B. R. (1991) *Infect. Immun.* **59,** 1755–1761
7. Gilleron, M., Himoudi, N., Adam, O., Constant, P., Venisse, A., Rivière, M., and Puzo, G. (1997) *J. Biol. Chem.* **272,** 117–124
8. Venisse, A., Fournié, J. J., and Puzo, G. (1995) *Eur. J. Biochem.* **231,** 440–447
9. Schlesinger, L. S., Hull, S. R., and Kaufmann, T. M. (1994) *J. Immunol.* **152,** 4070–4079
10. Sieling, P. A., Chatterjee, D., Porcelli, S. A., Prigozy, T. I., Mazzaccaro, R. J., Soriano, T., Bloom, B. R., Brenner, M. B., Kronenberg, M., Brenan, P. J., and Modlin, R. L. (1995) *Science* **269,** 227–230
11. Venisse, A., Berjeaud, J.-M., Chaurand, P., Gilleron, M., and Puzo, G. (1993) *J. Biol. Chem.* **268,** 12401–12411
12. Hunter, S. W., and Brennan, P. J. (1990) *J. Biol. Chem.* **265,** 9272–9279
13. Chatterjee, D., Lowell, K., Rivoire, B., McNeil, M., and Brennan, P. J. (1992) *J. Biol. Chem.* **267,** 6234–6239
14. Brennan, P. J., and Nikaido, H. (1995) *Annu. Rev. Biochem.* **64,** 29–63
15. Venisse, A., Rivière, M., Vercauteren, J., and Puzo, G. (1995) *J. Biol. Chem.* **270,** 15012–15021
16. Delmas, C., Gilleron, M., Brando, T., Vercellone, A., Gheorgiu, M., Rivière, M., and Puzo, G. (1997) *Glycobiology* **7,** in press
17. Bordier, C. (1981) *J. Biol. Chem.* **256,** 1604–1607
18. Ciucanu, I., and Kerek, F. (1984) *Carbohydr. Res.* **131,** 209–217
19. Schnitger, H., Papenberg, K., Ganse, E., Czok, R., Bücher, T., and Adam, H. (1959) *Biochem. Z.* **332,** 167–185
20. Ferguson, M. A. J., Haldar, K., and Cross, G. A. M. (1985) *J. Biol. Chem.* **260,** 4963–4968
21. Guttman, A., Chen, F. T. A., Evangelista, R. A., and Cooke, N. (1996) *Anal. Biochem.* **233,** 234–242
22. Lerner, L., and Bax, A. (1986) *J. Magn. Res.* **69,** 375–380
23. Shaka, A. J., Barker, P. B., and Freeman, R. (1985) *J. Magn. Res.* **64,** 547–552
24. Marion, D., and Wüthrich, K. (1983) *Biochem. Biophys. Res. Commun.* **113,** 967–974
25. Thurnher, M., Ramoner, R., Gastl, G., Radmayr, C., Böck, G., Herold, M., Klocker, H., and Bartsch, G. (1997) *Int. J. Cancer* **70,** 128–134
26. Sweet, D. P., Shapiro, R. H., and Albersheim, P. (1975) *Carbohydr. Res.* **40,** 967–974
27. Wang, Y., and Hollingsworth, R. I. (1995) *Anal. Biochem.* **225,** 242–251
28. Glushka, J., Cassels, F. J., Carlson, R. W., and Van Halbeek, H. (1992) *Biochemistry* **31,** 10741–10746
29. Mühlradt, P. F., Wray, V., and Lehmann, V. (1977) *Eur. J. Biochem.* **81,** 193–203
30. Budzikiewicz, H., and Rullkötter, J. (1973) *Z. Naturforsch.* **28c,** 499–504
31. Leopold, K., and Fischer, W. (1993) *Anal. Biochem.* **208,** 57–64
32. Cella, M., Sallusto, F., and Lanzavecchia, A. (1997) *Curr. Opin. Immunol.* **9,** 10–16
33. Schlesinger, L. S., Kaufmann, T. M., Iyer, S., Hull, S. R., and Marchiando, L. K. (1996) *J. Immunol.* **157,** 4568–4575
34. Hunter, S. W., Rivoire, B., Mehra, V., Bloom, B. R., and Brennan, P. J. (1990) *J. Biol. Chem.* **265,** 14065–14068
35. Adam, O., Vercellone, A., Paul, F., Monsan, P. F., and Puzo, G. (1995) *Anal. Biochem.* **225,** 321–327
36. Khoo, K.-H., Dell, A., Morris, H. R., Brennan, P. J., and Chatterjee, D. (1995) *J. Biol. Chem.* **270,** 12380–12389
37. Zhang, Y., Broser, M., Cohen, H., Bodkin, M., Law, K., Reibman, J., and Rom, W. N. (1995) *J. Clin. Invest.* **95,** 586–592
38. Guo, L., Lim, K. B., Gunn, J. S., Bainbridge, B., Darveau, R. P., Hackett, M., and Miller, S. I. (1997) *Science* **276,** 250–253